Quantum chaos and two exactly solvable second-quantized models

W.-H. Steeb and C. M. Villet

Department of Physics, Rand Afrikaans University, P.O. Box 524, Johannesburg 2000,
Republic of South Africa

A. Kunick

Kraftwerkunion Rechenzentrum, D-8520 Erlangen,
West Germany

Two exactly solvable second-quantized models, namely, a one-fermion–one-boson model and the four-point Hubbard model, are presented. The connection with quantum chaotic behavior is discussed.

A large number of authors (compare Refs. 1–5 and references therein) have studied the interrelation between classical Hamiltonian systems which show chaotic behavior above a threshold value E_c and the corresponding quantum system. In most cases the standard quantization has been used. Various approaches have been applied to "define" what we understand by "quantum chaos." Among others, there are the method of avoiding energy-level crossings, the study of the sensitivity of energy eigenvalues to perturbations, the statistical analysis of fluctuations in the spectral sequences, the structure of the eigenvectors, the sequence of level spacings, and the distributions of nearest-neighbor spacings. When we consider the method of distribution of the nearest-neighbor spacings we find that in the regular case (i.e., the classical case is integrable) the energy eigenvalues are distributed randomly, leading to a Poisson-type of distribution function.[3] The most important exceptions are coupled harmonic oscillators. When the classical system is almost integrable the quantized version also leads to a Poisson-type of distribution function. A regular spectrum (quantum chaos) occurs when the energy levels are correlated, resulting in a repulsion of adjacent levels. The nearest-neighbor-spacings distribution function peaks at a finite value and exhibits the typical feature of a Wigner function. In this case the classical system shows chaotic behavior. Another approach for studying quantum chaos is to plot graphs of level spacings $\Delta E_n = E_{n+1} - E_n$. This approach was proposed by Hirooka, Yotsuya, Kobayashi, and Saito.[6] However, Farrelly[7] and Berry[8] demonstrated that this representation is not unique. They emphasize that the irregularity is in the wave functions and matrix elements.

In the present paper we study two exactly solvable models. We consider a one-fermion–one-boson model for a magnetic elastic system[9] and the half-filled four-point Hubbard model. For both models there is no classical analog. Nevertheless, we can look for the connection with quantum chaos.

For the one-fermion–one-boson system we are able to calculate the spectrum exactly. Consequently, we can study the distribution of the nearest-neighbor spacings. Owing to the appearance of Bose operators the number of the energy levels is infinite. We are also able to calculate the energy spectrum exactly for the four-point Hubbard model. Since only Fermi operators appear, the number of energy levels is finite. It is known[10] that in the case of the linear chain with cyclic boundary conditions, the ground-state energy of

the Hubbard model can be calculated exactly for $N \to \infty$, $N_e \to \infty$, and $N_e/N = 1$. (N is the number of lattice sites; N_e is the number of electrons.) Lieb and Wu[10] used the multicomponent Bethe ansatz. For this half-filled case Takahashi[11] calculated the thermodynamic quantities under certain assumptions. If these assumptions hold, then one calls this model integrable. Recently, Bariev and Kozhinov[12] demonstrated that the one-dimensional Hubbard model cannot be understood in terms of the quantum inverse-scattering method. There are a number of multisublattice integrable systems, the exact solution of which can be obtained using the multicomponent Bethe ansatz, which, however, cannot (yet) be understood in terms of the quantum inverse-scattering method. Thus it would be interesting to compare with calculations concerning quantum chaos.

The one-fermion–one-boson model with Hamiltonian operator

$$\hat{H} = wb^*b + Jc^*c + a(b + b^*)(c + c^*) \tag{1}$$

cannot be solved exactly (compare Refs. 9 and 13–15). Notice that $c^* = \sigma^+/2$ and $c = \sigma^-/2$. It can be proved that $\hat{H}$ commutes with the parity operator $\hat{P} = \exp[i\pi(b^*b + c^*c)]$. In the so-called rotating-wave approximation ($J \cong w$, $a \ll J$), the Hamiltonian operator takes the form

$$\hat{H}_r = wb^*b + Jc^*c + a(b^*c + bc^*) . \tag{2}$$

This operator commutes with $\hat{P}$ and $\hat{N} = c^*c + b^*b$. The eigenvalue problem can easily be solved. We find

$$\{0, \ J/2 + w/2 + nw \pm [\tfrac{1}{4}(J - w)^2 + a^2(n + 1)]^{1/2}\} , \tag{3}$$

where $n = 0, 1, 2, \ldots$. In Fig. 1 we have plotted the distribution of nearest-neighbor spacings where $w = J = 0.5$ and $a = 0.1$. We have taken into account the first 4000 levels. The distribution cannot be identified with a pure Poisson distribution or with a pure Wigner distribution. However, the typical feature of a Wigner distribution, namely, that $P(S) \to 0$ as $S \to 0$, is not present. Consequently, we do not identify the system with quantum chaos. Figure 2 shows ΔE_n as a function of n for $w = J = 0.5$ and $a = 0.1$.

For the Hamiltonian (1) we are not able to exactly calculate the eigenvalues. Nevertheless, we can calculate the matrix representation. Then we are forced to truncate the matrix and numerically calculate the eigenvalues of this finite matrix. For our numerical calculation we take the first 400
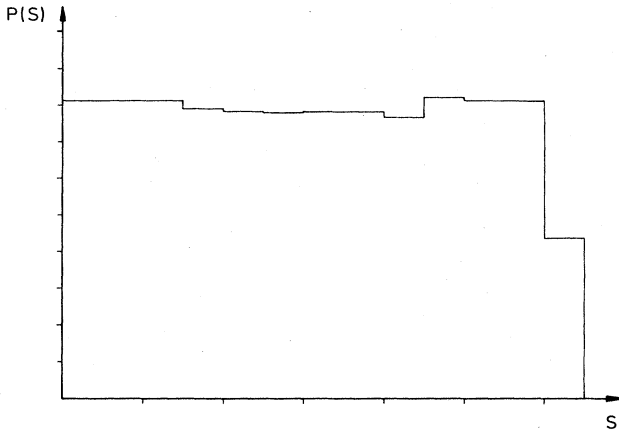
BRIEF REPORTS

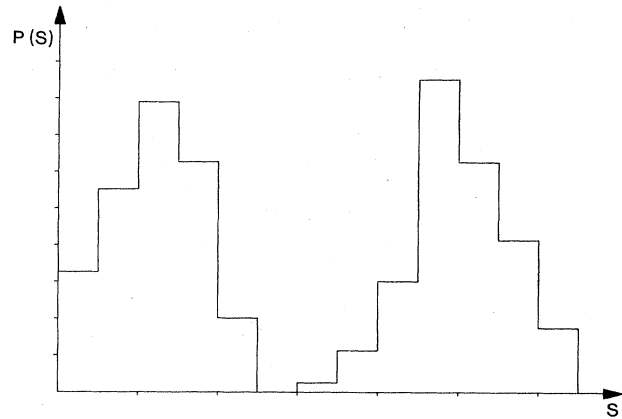FIG. 1. Nearest-neighbor-spacings histogram for the energy levels (3) for $w = J = 0.5$ and $a = 0.1$.

FIG. 3. Nearest-neighbor-spacings histogram for the first 400 energy levels for the Hamiltonian (1) $w = J = 0.5$, $a = 0.1$.

energy levels into account. Figure 3 shows the histogram.

Let us now study the four-point Hubbard model with cyclic boundary conditions

$$\hat{H} = t \sum_{i=1}^{4} \sum_{\Delta = \pm 1} \sum_{\sigma} c_{i+\Delta\sigma}^{*} c_{i\sigma} + U \sum_{i=1}^{4} n_{i\uparrow} n_{i\downarrow} \quad , \tag{4}$$

where $c_0 = c_4$ and $c_1 = c_5$. Note that $\hat{H}$ commutes with

$$\hat{N}_e = \sum_{i\sigma} c_{i\sigma}^{*} c_{i\sigma}$$

and

$$\hat{S}_z = \sum_{i} (c_{i\uparrow}^{*} c_{i\uparrow} - c_{i\downarrow}^{*} c_{i\downarrow}) \quad .$$

The Hamiltonian (4) admits the C_{4v} point-group symmetry.

Since cyclic boundary conditions are imposed, we can transform the Hamiltonian (4) into momentum space. We find that

$$\hat{H} = \sum_{k} \sum_{\sigma} \epsilon(k) c_{k\sigma}^{*} c_{k\sigma}$$
$$+ (U/N) \sum_{k_1, k_2, k_3, k_4} \delta(k_1 - k_2 + k_3 - k_4) c_{k_1\uparrow}^{*} c_{k_2\uparrow} c_{k_3\downarrow}^{*} c_{k_4\downarrow} \quad , \tag{5}$$

where

$$k \in [-\pi/2, \ 0, \ \pi/2, \ \pi \ (\mathrm{mod} \ 2\pi)]$$

and $\epsilon(k) = 2t \cos k$. Since $\hat{H}$ commutes with the total momentum operator

$$\hat{P} = \sum_{k} k (c_{k\uparrow}^{*} c_{k\uparrow} + c_{k\downarrow}^{*} c_{k\downarrow}) \quad , \tag{6}$$

it follows that we can classify the eigenfunctions of $\hat{H}$ as belonging to a subspace of equal total momentum, namely, $P = -\pi/2, \ 0, \ \pi/2,$ and π. Since $\hat{H}$ and $\hat{P}$ are invariant under spin reversal, it is possible to define an operator $\hat{S}$ which satisfies $\hat{S}^2 = I$. The eigenvalues of $\hat{S}$ are obviously $S = \pm 1$. Thus we can classify the eigenstates as belonging to negative or positive spin parity. In the case $N_e = 4$ and $S_z = 0$ we find that the dimension of our Hilbert space is given by $\dim \hbar = 36$. For the dimensions of the subspaces with $P = -\pi/2, \ 0, \ \pi/2,$ and π we obtain 8, 10, 8, 10. Now a straightforward calculation leads to ($K = t/U$,
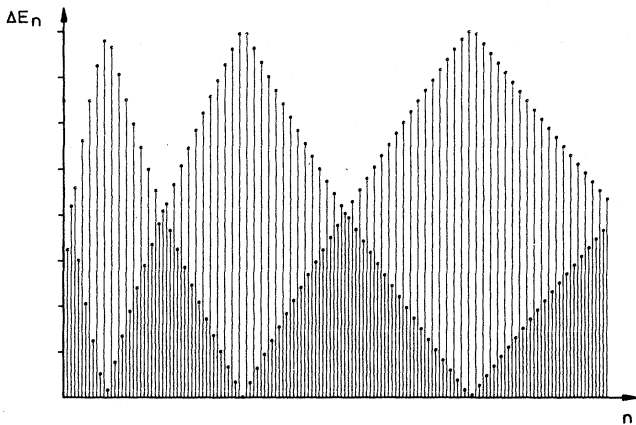

FIG. 2. Energy-level spacings $\Delta E_n = E_{n+1} - E_n$ vs n (150 levels) for $w = J = 0.5$ and $a = 0.1$.
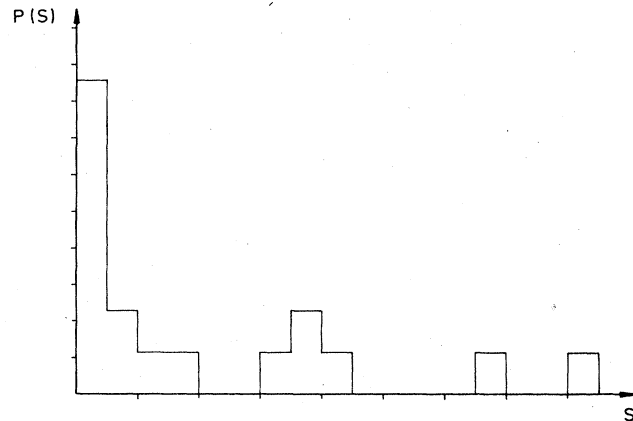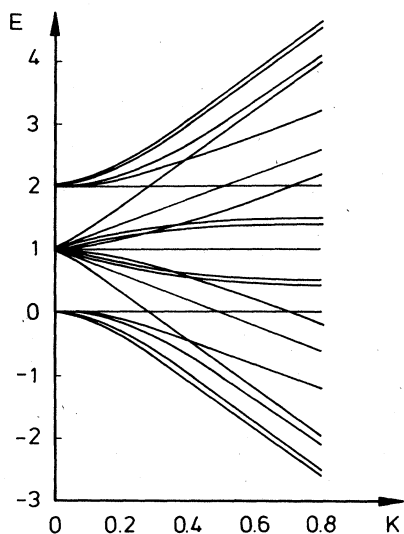

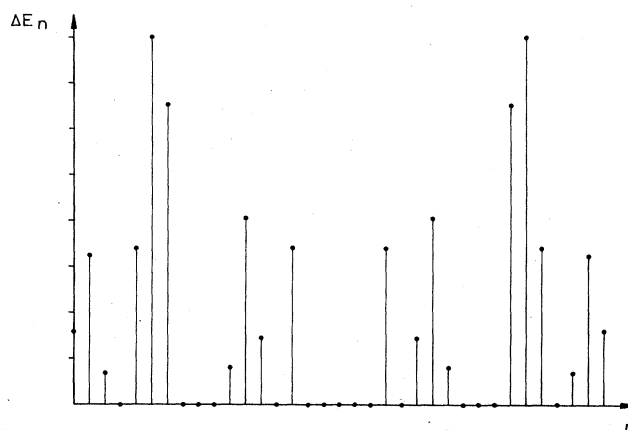FIG. 4. Nearest-neighbor-spacings histogram for the four-point Hubbard model ($K = 0.2$).

FIG. 5. Energy level vs K for the four-point Hubbard model.

FIG. 6. Energy-level spacings $\Delta E_n = E_{n+1} - E_n$ for the four-point Hubbard model ($K = 0.2$).

$E \to E/U)$

$$E(E-1)^3[E^3 - 4E^2 + E(5 - 16K^2) + 24K^2 - 2]$$

$$\times [E^3 - 3E^2 + 2E(1 - 8K^2) + 24K^2] = 0 \ ,$$

$$[(E-1)^2 - 4K^2]^2(E^2 - 3E + 2 - 4K^2)(E^2 - E - 4K^2) = 0 \ ,$$

$$[(E-1)^2 - 4K^2]^2(E^2 - 3E + 2 - 4K^2)(E^2 - E - 4K^2) = 0 \ ,$$

$$(E-1)^3(E-2)[E^3 - 3E^2 + 2E(1 - 8K^2) + 8K^2]$$

$$\times [E^3 - 2E + E(1 - 16K^2) + 8K^2] = 0 \ . \quad (7)$$

We see that the eigenvalue $E = 1$ is sixfold degenerate. The number of energy levels is low, so that a reliable statistical test is doubtful. Nevertheless, in Fig. 4 we have plotted the distribution for $K = 0.2$. We can identify it with a Poisson distribution. The different energy levels as a function of K have been plotted in Fig. 5. We find crossings of energy levels. This is another indication for integrability. Figure 6 shows ΔE_n as a function of n for $K = 0.2$, where we have included the degeneracy.

It should be worthwhile to study the Hubbard model with more than four lattice sites so that the number is sufficiently large to perform a reliable statistical test. For arbitrary N ($N = N_e$, $S_z = 0$) the dimension of the Hilbert space is

given by

$$\dim \mathscr{A} (N_e = N, \ S_z = 0) = \sum_{n=0}^{N/2} \frac{N!}{(N/2 - n)!(N/2 - n)!}$$

$$= \left[\binom{N}{N/2} \right]^2 \ . \quad (8)$$

For $N = 6$ we obtain $\dim \mathscr{A}(N_e = N, \ S_z = 0) = 400$. Consider cyclic boundary conditions. For the dimensions of the subspaces with $P = -2\pi/3, \ -\pi/3, \ 0, \ \pi/3, \ 2\pi/3$, and π we find 66, 68, 66, 66, 68. We have studied the subspace with $P = 0$. Here, too, we find a Poisson distribution. The question remains open whether or not we find Poisson distribution for higher values of N.

In the discussion of quantum chaos one starts from a classical Hamiltonian which can be integrable, almost integrable, or chaotic (due to the parameter values or the energy value). Then the Hamiltonian is quantized and the spectrum is calculated. Thus we have the behavior of the classical systems as a guide to the behavior to be expected in the quantum version. If there is no classical analog, then we can ask whether the system can be solved with the help of the Bethe ansatz or the quantum inverse-scattering method. We conjecture that models which can be solved via the inverse-scattering method or with the help of the Bethe ansatz do not show quantum chaos as indicated, e.g., by a Wigner distribution of nearest-neighbor spacings.

[1]I. C. Percival, Adv. Chem. Phys. **36**, 1 (1977).
[2]M. V. Berry, J. Phys. A **10**, 2083 (1977).
[3]M. V. Berry and M. Tabor, Proc. R. Soc. London, Ser. A **356**, 375 (1977).
[4]P. Pechukas, Phys. Rev. Lett. **51**, 943 (1983).
[5]R. A. Pullen and A. R. Edmonds, J. Phys. A **14**, L319 (1981).
[6]H. Hirooka, Y. Yotsuya, Y. Kobayashi, and N. Saito, Phys. Lett. **101A**, 115 (1984).
[7]D. Farrelly, Phys. Lett. **104A**, 63 (1984).

[8]M. V. Berry, Phys. Lett. **104A**, 306 (1984).
[9]F. Leyvraz and P. Pfeifer, Helv. Phys. Acta **50**, 857 (1977).
[10]E. H. Lieb and F. Y. Wu, Phys. Rev. Lett. **20**, 1445 (1968).
[11]M. Takahashi, Prog. Theor. Phys. **47**, 69 (1972).
[12]R. Z. Bariev and Yu. V. Kozhinov, Physica A **127**, 316 (1984).
[13]S. Schweber, Ann. Phys. (N.Y.) **41**, 205 (1967).
[14]S. Swain, J. Phys. A **6**, 1919 (1973).
[15]F. T. Hioe and E. W. Montroll, J. Math. Phys. **16**, 1259 (1975).